

Infrared Spectroscopy Analysis of Oxyhydroxides as Intermediate Species in the Formation of Iron Oxides-Silica Xerogels

S. Ponce-Castañeda, J.R. Martínez, S. Palomares-Sánchez, Facundo Ruíz, O. Ayala-Valenzuela, J.A. Matutes-Aquino

Abstract

A detailed infrared spectroscopy analysis in the 2500 to 3800 cm^{-1} region has been used to study the formation of species in samples of iron oxides embedded in silica xerogel matrix. We report the presence of α , β , and γ forms of iron oxyhydroxides as intermediate species in the formation of $\alpha\text{-Fe}_2\text{O}_3$, $\gamma\text{-Fe}_2\text{O}_3$ and $\epsilon\text{-Fe}_2\text{O}_3$ starting from three different iron precursors: iron nitrate, iron chloride and nanometric Fe particles prepared by chemical reduction. Our results show that under thermal dehydration α and γ forms of iron oxyhydroxides transform into hematite and maghemite, respectively, whereas the β form transform to the $\epsilon\text{-Fe}_2\text{O}_3$ without going through an intermediate iron oxide phase.

Keywords: sol-gel, infrared (IR) spectroscopy, vibrating sample magnetometry, composites, oxyhydroxides.

Introduction

The study of systems of iron oxides particles embedded in inert matrixes has received a lot of attention due to their potential applications in magnetic recording, magnetic refrigeration, etc [1–3]. An excellent supporting medium for magnetic iron oxide particles has been the SiO_2 matrix obtained using the sol-gel preparation method [4–6]. The formation of iron oxides species depends on the intermediate oxyhydroxides

formed in the initial stages of the formation process of composites of iron oxides in silica.

Iron oxides and iron oxyhydroxides find applications as pigments, catalyst, absorbent and magnetic storage media [7, 8]. Their properties can change dramatically when the particle size is confined in the nanometer-size range. Amorphous or crystalline silica matrixes can be used to limit the growth of the particles resulting in isolated iron oxide/oxyhydroxide units.

Among the preparation method for this kind of materials, the sol-gel technique offers some advantages.

With this preparation method supported species are effectively incorporated into the oxide network and may yield more stable catalysts than those prepared by conventional methods [9]. The classic sol-gel process to preparing metal oxide glasses, involves hydrolysis and polycondensation of alkoxides, e.g., tetraethyl orthosilicate (TEOS).

In a previous work we have reported that the final iron oxides species precipitated into the silica matrix, strongly depends on the oxyhydroxides species formed at early stages [10]. In this paper we study the formation of oxyhydroxides species and their evolution to iron oxides species under heat treatments using infrared spectroscopy.

Experimental Methods

The starting solutions for the formation of silica xerogel composites were prepared by mixing tetraethyl orthosilicate (TEOS), water, and ethanol. The mole ratios of ethanol to TEOS and water to TEOS were 4:1 and 11.67:1, respectively. Separately, amounts of $\text{Fe}(\text{NO}_3)_3 \cdot 9\text{H}_2\text{O}$, $\text{FeCl}_3 \cdot 6\text{H}_2\text{O}$ and Fe-O particles were added to the

solution at such amount that the metal oxide concentration, assuming full metal oxidation, is 30% wt. of the final dried powders.

The nitrates and chlorides used as precursors of iron species were $\text{Fe}(\text{NO}_3)_3 \cdot 9\text{H}_2\text{O}$ and $\text{FeCl}_3 \cdot 6\text{H}_2\text{O}$, respectively. For their incorporation into the SiO_2 matrix, the iron nitrate and iron chloride were dissolved in water; the hydration from chloride and nitrate is included in the above mentioned water:TEOS ratio. For the nanometric Fe particles, after their preparation the particles were added to the ethanol. In all cases, homogenous solutions of all components were obtained by mixing water, ethanol and TEOS for about 15 min. using a magnetic stirring.

Nanometric Fe particles were prepared by using as reduction agent, a 0.3 M aqueous solution of NaBH_4 . The precursor employed in the synthesis of metal iron was a 0.05M aqueous solution of $\text{FeCl}_3 \cdot 6\text{H}_2\text{O}$. Before adding the reduction solution, $\text{FeCl}_3 \cdot 6\text{H}_2\text{O}$ was solubilized in water adding HCl to adjust to 1.5 the pH of the solution. Then, NaBH_4 solution was slowly added, achieving Fe particles by mixing 200 ml of the NaBH_4 solution with 400 ml of $\text{FeCl}_3 \cdot 6\text{H}_2\text{O}$ solution at 25°C . The obtained product was washed in a Buchner funnel with methanol, then with acetone and finally kept in hexane. Size and morphology of the Fe particles were presented at a previous work [10].

Soft pieces of the gels were obtained after about 48 hr. Those pieces were ground to form a fine powder. For subsequent annealing, the samples were placed in an oven at the desired temperature for 30 min. in air.

Hereafter, the set of samples will be referred as: A, sample obtained starting from iron nitrate; B, sample obtained starting from iron chloride and C, sample obtained starting from Fe nanoparticles.

The Infrared (IR) spectra were measured in a FTIR spectrometer Nicolet System model Avatar 360, in the diffuse reflectance (DR) mode, mixing 0.05 gr. of powder sample with 0.3 gr. of KBr. Magnetic characterization was performed using a LDJ 9600 vibrating sample magnetometer at room temperature with $H_{\max} = 16$ KOe in order to obtain magnetic parameters such as saturation magnetization and coercivity. All measurements were performed at room temperature.

Results

The main infrared signature of OH groups is located in the 2500 to 3800 cm^{-1} region. In this region the silica and iron oxyhydroxides have strongly overlapping absorption. Of the various iron oxyhydroxides, α -FeO(OH) (goethite), β -FeO(OH) (akagenite) and γ -FeO(OH) (lepidocrocite) absorb in the above region [11]. This, when coupled with the fact that hydrogenbonded silanols themselves absorbs in this regions, further complicates the analysis.

In silica pure samples the bands in the range between 3600 and 4000 cm^{-1} are mainly due to overtones of combination of vibrations of Si OH or H₂O. The broad absorption band in between 3000 and 3600 cm^{-1} corresponds to the fundamental stretching vibrations of different hydroxyl groups, and is generally composed of a superposition of the following stretching modes: 3300 to 3500 cm^{-1} corresponds to adsorbed water; 3540 cm^{-1} corresponds to silanol groups linked to molecular water through hydrogen bonds; 3660 cm^{-1} corresponds to Si and OH pairs located at the

surface mutually linked by a hydrogen bond and internal Si OH. These bands tend to disappear under heat treatment.

It is possible to have bands due to overtones of the stretching and bending vibrations associated with the OH groups which are present in the structures of goethite and lepidocrocite. For goethite, the stretching and two bending fundamental vibrations occur at 3095 cm^{-1} , 890 cm^{-1} and 797 cm^{-1} , respectively. For lepidocrocite, the stretching fundamental is apparently doubled at 3390 cm^{-1} and 3125 cm^{-1} , and so is one of the bending fundamentals at 1161 cm^{-1} and 1026 cm^{-1} [12].

The 2500 to 3800 cm^{-1} IR absorption band can be resolved to obtain information about the changes in the silanol structure and the possibility of the presence of α and γ iron oxide hydroxides.

Figure 1 shows the infrared spectra in this region including a detailed analysis for the as-prepared samples of sets A, B and C. The figures show how the experimental curves can be decomposed in four absorption sub-bands.

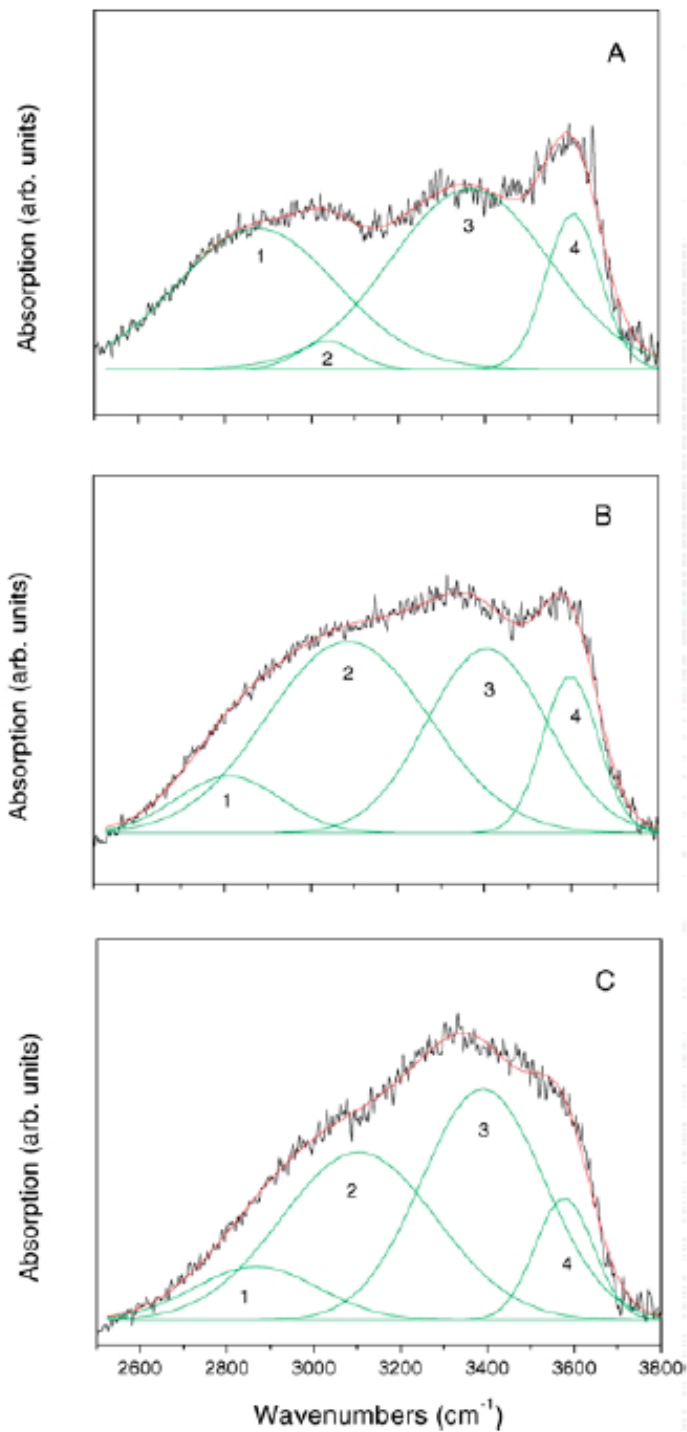


Figure 1. IR analysis in the spectral region of 2500 to 3800 cm^{-1} for as-prepared Fe-doped SiO_2 samples using three different precursor A) iron nitrate, B) iron chloride, and C) nanometric Fe particles.

The smooth line corresponds to the sum of all four bands in which experimental curve has been decomposed. As it is well known, in a deconvolution analysis, the positions of the absorption sub-bands are very sensitive to how the baseline is defined, so that variation in sub-bands position could be due to this difficulty. However, in our case the observed variation, in the sub-bands positions, is ascribed mainly to the presence of different iron oxide species. The founded sub-bands, after the deconvolution analysis, for the set of studied samples coincide with the peaks assigned to the hydrogen-bonded silanol.

For the sample A we obtain four band centred at about 2875, 3036, 3365 and 3602 cm^{-1} . The features, area and intensity, of the 3036 cm^{-1} band are very small compared with the band centred at 3365 cm^{-1} , band (3).

For the sample B the sub-bands are located at about 2810, 3084, 3405, and 3597 cm^{-1} . For this sample we observed that the band (2), at 3084 cm^{-1} , has comparable features respect to the band at 3405 cm^{-1} , band (3). Whereas for the sample C the sub-bands are located at 2867, 3103, 3389 and 3577 cm^{-1} . For this case the features of the band at 3103 cm^{-1} , band (2), are similar than the sample B case.

The position of sub-band (3) for the different samples A, B, and C, shows a significant variation. This variation is associate with the iron oxide precursor, added to the initial solutions of the gels. For sample B, the chloride salt retains the water hydration retarding the hydrolysis process; whereas case A due to the high solubility of nitrates the hydratation water from the salts allows a total hydrolysis of TEOS molecules; And finally for case C we have a normal TEOS hydrolysis process. [3, 10].

In the range from 2800 to 3800 cm^{-1} the silica and iron oxyhydroxides have strongly overlapping absorption; however is possible to assign a stretching fundamental vibration for goethite at about 3095 cm^{-1} [12]. The analysis of the band (2) and the measure of its relative intensity respect to band (3) suggests, at first glance, that the intermediate oxide hydroxide in the samples B and C is $\alpha\text{-FeO(OH)}$ (goethite). This assignment is corroborated by the detection of a peak at about 890 cm^{-1} (not showed in figures) in both set of samples; for the sample C the main stretching band expands from 828 to 1273 cm^{-1} and in the sample B this contribution appears in the silanol band from 870 to 994 cm^{-1} . This result is in agreement with previous results of Uv-Visible spectroscopy [10]. For the sample A is difficult to assign a oxyhydroxide phase, however we can see that the intermediate oxide hydroxide is unlikely to be $\alpha\text{-FeO(OH)}$.

Figures 2 to 4 show the IR spectra for the set of samples A, B and C under different heat treatments, from these results we can follow the evolution of the dehydration process and the iron oxyhydroxides phases as well. In Fig. 2 we can see how the intensities of sub-bands, for sample A, varies as a function of temperature. In particular the variation in the intensity of sub-band (2) is noticeable. The position of the band (2) in the heat treated samples shift to 3124 cm^{-1} ; this band was originally located at 3036 cm^{-1} for the asprepared sample. This position is the same for samples heat treated at 200°C to 600°C. This sub-band is assigned to $\gamma\text{-FeO(OH)}$ (lepidocrocite) [13].

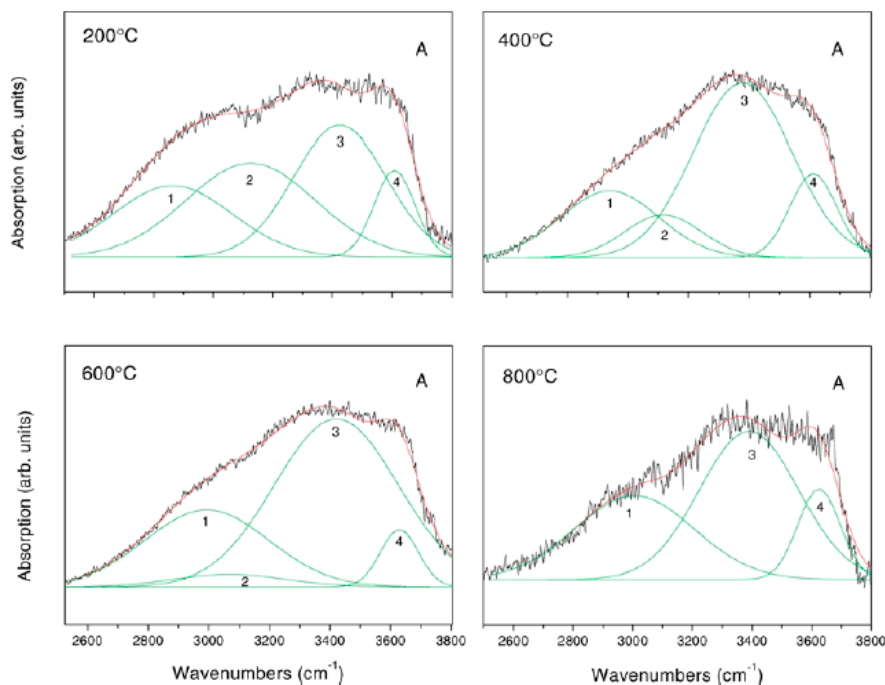


Figure 2. IR analysis in the spectral region of 2500 to 3800 cm^{-1} for sample A annealed in air at (a) 200°C, (b) 400°C, (c) 600°C, and (d) 800°C.

This fact and the results of Uv-visible spectroscopy reported previously [10], indicate us that the first oxyhydroxide phase for the sample A case is lepidrococite and is formed at temperatures lower than 200°C. The relative intensity of the band (2), for the sample A heat treated at 200°C, is comparable with the intensity of the band (3). This intensity diminish according with the increase of temperature. When the samples were heat treated form 200°C to 800°C the intensity of subband (2) decrease monotonically from 0.06 (200°C) to 0.0023 (600°C), disappearing at 800°C, indicating a reduction in the lepidrococite phase. This reduction is accompanied with the appearing of the maghemite phase, according with XRD previous results [10]. For the sample heat treated at 800°C the band (2) is absent, for this temperature the lepidrococite phase disappears and the maghemite phase is completely formed [10].

Figure 3 shows the decomposed spectra for the sample B heat treated at 200°C and 400°C. From the figure we can observe that the intensity of the band (2) diminishes with respect to the band (3). For the sample heat treated at 400°C the contribution peak of the sub-band (2) is insignificant. It is known that the oxide phase of hematite is present at temperatures of about 400°C in this kind of samples [10, 14]. We can conclude that the goethite phase transforms to the iron oxide phase of hematite.

For the sample C (Fig. 4), the heat treatment produces a noticeable decrease in the intensity of the band (2), when compared with the as-prepared sample, this sub-band disappears at temperatures of 600°C. This diminution indicates to us the evolution of the goethite phase. This phase is maximum in the as-prepared sample and disappears at temperatures of 600°C or higher.

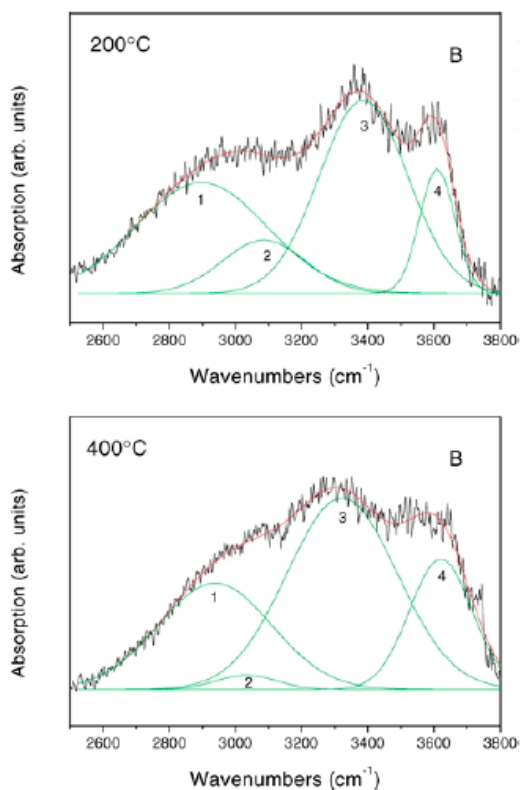


Figure 3. IR analysis in the spectral region of 2500 to 3800 cm^{-1} for sample B annealed in air at (a) 200°C and (b) 400°C.

The magnetization curves for sample A, at the indicated temperatures, are shown in Fig. 5. The curves at temperatures from 200°C to 600°C are not resolved in the indicated scales, their saturation magnetization is of the order of 0.007 emu/g. From Figs. 1 and 2 we see that the lepidocrocite phase is presents in heattreated samples at the range of temperatures above mentioned. At 800°C we detect the disappearance of lepidocrocite and the presence of γ -Fe₂O₃ phase, this fact is in relationship with the dramatic increase in magnetic properties; the magnetization saturation grows to above 1 emu/g. At 1000°C a change of phase occurs according with previous report [10], the new phase is ϵ -Fe₂O₃ which is derived from the akagenite phase formed at temperatures above 800°C [10]. The coercivity and saturation magnetization values are increased 6 and 3 times, respectively respect to the curve at 800°C.

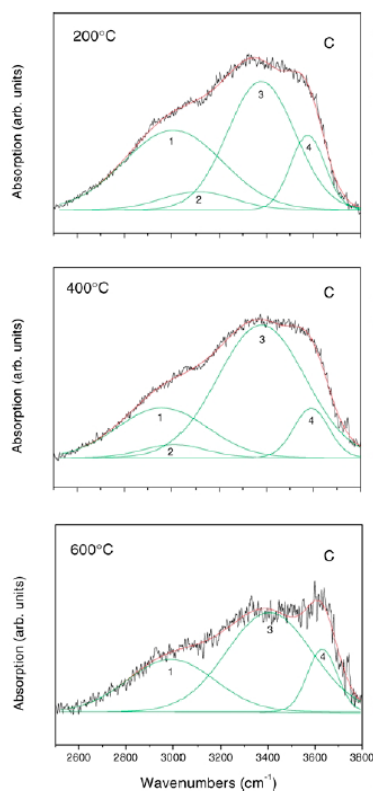


Figure 4. IR analysis in the spectral region of 2500 to 3800 cm⁻¹ for sample C annealed in air at (a) 200°C, (b) 400°C, and (c) 600°C.

The magnetic parameters for the sample heat treated at 1100°C show changes in their expected comportment. This situation is related to a structural change produced by the interaction of the iron oxide nanocluster with the silica gel matrix. A noticeable increase in the coercivity accompanied by a diminishment in the saturation magnetization is observed at this temperature. The reduction of this value may be caused by noncolinearity of the magnetic moments at the surface of the nanoparticles, resulting in a decrease of the saturation magnetization for small particles [15].

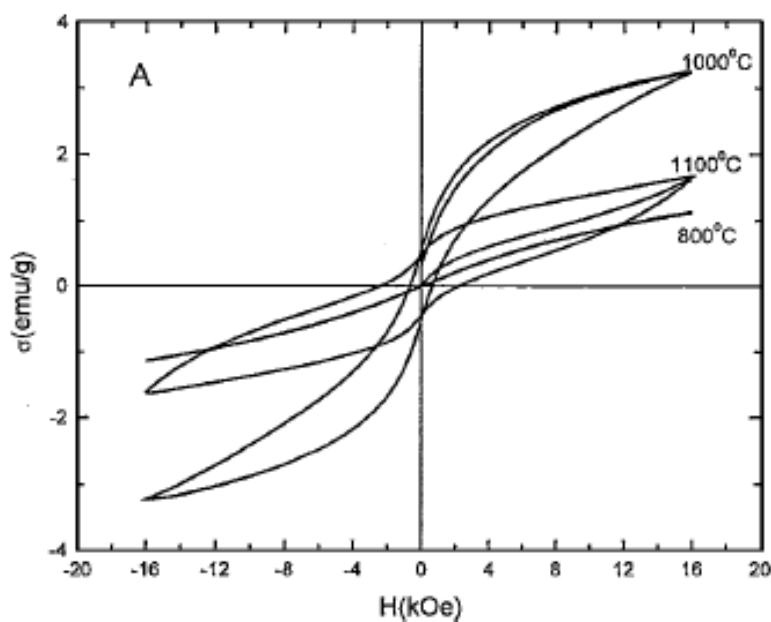


Figure 5. Hysteresis loops of the sample A heat treated at 800°C, 1000°C and 1100°C.

The saturation magnetization is reduced to about 1.6 emu/g, 49% lower than for the sample heat treated at 1000°C. The coercivity value measured for the 1100°C heat treated sample is 2510 Oe, whereas the value measured in the 1000°C heat treated sample is 730 Oe. We believe that the iron oxide phase-glass interface could strongly influence the coercivity and saturation magnetization of our nanocomposites. Since our samples contain very small particles, a large fraction of ions is at or near the surface so

that the interaction between the iron oxide particles and the silica matrix may play a determinant role.

Figure 6 shows the hysteresis loop for sample B. We can observe the paramagnetic behaviour of the sample heat-treated at 200°C; at this temperature, the iron oxide is still not present, only the goethite oxyhydroxide phase is present. From the figure we observed that an evident change in the coercivity occurs when the sample has been heat treated from 200°C to 400°C. The coercivity value for the sample heat treated at 400°C is about 2874 Oe. At this temperature occurs a phase transformation from goethite oxyhydroxide phase to hematite phase. The magnetic parameters for the sample heat treated at 1100°C show a change in their expected comportment. This situation could be related to a structural change produced by the interaction of the hematite nanocluster within the silica gel matrix. It is interesting to observe the constricted hysteresis loop which is characteristic of self-magnetic annealed materials, when they are annealed at temperatures higher than T_c . This fact can be explained by considering the effect of directional order on domain walls. For this temperature we have reported the presence of partial crystalization of the silica matrix in cristobalite [10].

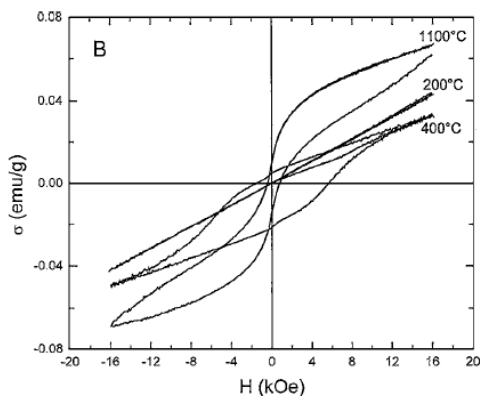


Figure 6. Hysteresis loops of the sample B heat treated at 200°C, 400°C and 1100°C.

In this case the coercivity reduce to 450 Oe, Figure 7 show the magnetization curve for sample C. In this case we obtain simultaneously an iron oxide species (maghemite) and the goethite oxyhydroxide phase for the as-prepared sample. The comportment of the magnetic curves do not present dramatic changes, contrary of the sample A case. Changes in the saturation magnetization depends of the iron oxide size variations.

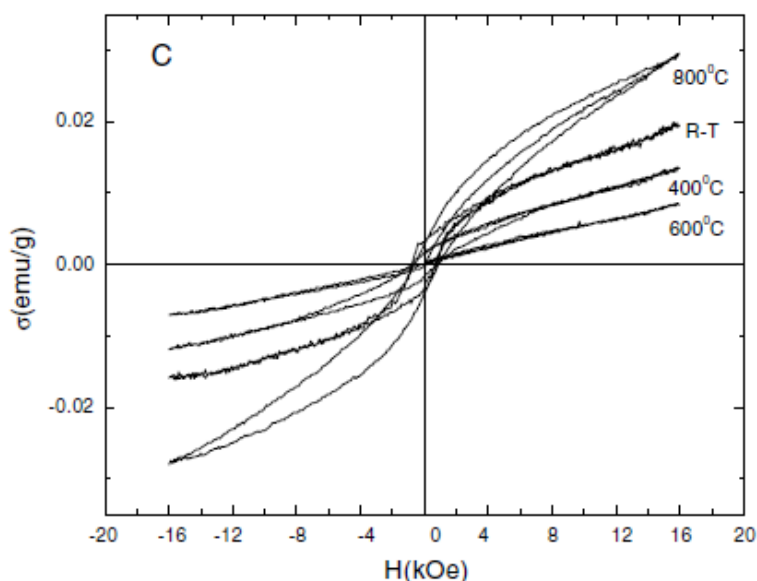


Figure 7. Hysteresis loops of the sample C at room temperature and heat treated at 400°C, 600°C and 800°C.

However, we can observe that at 600°C the coercivity is reduced from about 900 Oe to 250 Oe. This reduction coincides with the disappearance of the goethite phase. At 800°C a growth in the magnetic properties occurs due to the presence of the hematite phase [10].

Discussion

The reaction of iron clusters with surface silanols is mediated through an oxyhydroxide. The presence of these iron oxide hydroxides was examined by infrared

spectroscopy in the 2500 to 3800 cm^{-1} range, where silica and iron oxyhydroxides have strongly overlapping absorption bands. The broad IR absorption bands in this range were resolved to obtain important information about the changes in the silanol structure and the contribution of oxyhydroxides.

The presence of the Si (OH) groups even after the treatment at 600°C is contrary to the annealing behavior of similar samples without iron oxides. In the silica pure samples case, the Si (OH) groups gradually disappear with the increase in the annealing temperature, being basically removed for temperatures around 600°C. Besides the broad O H feature in the 3500 cm^{-1} region, for the pure sample, was stronger in the iron oxide-silica samples. This difference can be attributed to variations in the surfaces hydroxyl content, a characteristic that is expected to affect the use of this material for different applications. Parler et al. [16] has reported two additional peaks located at 315 and 3030 cm^{-1} in the spectra of silicon-iron system. In agreement with Parler additional peaks for the iron oxide-silica samples appear in this region; their position depends of the iron precursor and the heat treatment temperature. These peaks, labelled as band (2), are assigned to the presence of oxyhydroxides species.

In the deconvolution process the band (2) suffers dramatic changes in its intensity and area, and for the sample A in its position, whereas for the other bands only little changes are observed. The assignment for the bands (3) and (4) corresponds to hydrogen-bonded silanol, and adsorbed water. In the silica pure case the variation of the bands is uniform and for temperatures above 600°C they disappear. The comportment of the band (2) for the set of samples analysed suggest that hydroxyl groups are linked to monoxide iron forming oxyhydroxides groups which absorb at the

range from 3050 to 3130 cm^{-1} [12–14]. The iron precursor used determines the position of this band and the kind of oxyhydroxide produced. For the sample A the position corresponds to lepidocrocite [12], whereas for the set of samples B and C the position corresponds to goethite [12, 13]. The variation in intensity for the band (2) give us information about the concentration of species. When the band disappears a phase transformation occurs. In our case the elimination of lepidocrocite conduces to the appearance of maghemite and when the goethite disappears hematite appears.

For the sample C we have simultaneously the presence of maghemite and goethite phase in the temperature range from room temperature to about 600°C and then, due to the presence of goethite, a retardation of the maghemite to hematite phase transition occurs. This retardation could be due to the presence of strong hydrogen-bonded interaction between the maghemite phase and silica surface according with Ramesh et al. [14], which promotes a slowly thermal dehydration of goethite.

The thermal dehydration of pure iron oxyhydroxides to iron oxides shows that α and γ forms of iron oxyhydroxides on thermal dehydration transform into hematite and maghemite, respectively, whereas the β form transforms to $\epsilon\text{-Fe}_2\text{O}_3$ without going through an intermediate iron oxide phase. A schematic diagram showing the possible thermal dehydration products during the dehydration of iron oxyhydroxides is depicted in Fig. 8.

These results agree partially with the schematic diagram obtained by Ramesh et al. [14]. They report that akagenite, β form of iron oxyhydroxide transforms into hematite. In our case this phase transforms to $\epsilon\text{-Fe}_2\text{O}_3$ phase [10]. It is reported that the transformation to hematite phase is favoured under dry condition [14]. We obtain that at

high temperatures the presence of group OH is evident and then akagenite phase appears, as in sample A case, transforming later in ϵ - Fe_2O_3 .

The magnetic properties for the set of samples in the dehydration process suffer evident changes due to the phase transformation of oxyhydroxides species to iron oxides species. The samples show a paramagnetic compartment when a oxyhydroxide phase is present, this is noticeable in Fig. 6, for the sample B case.

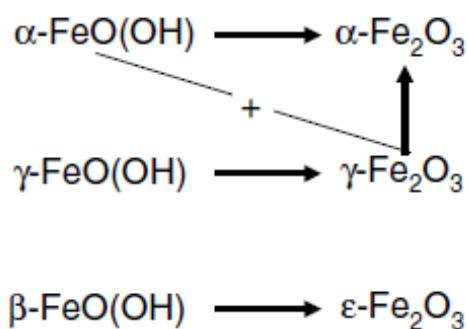


Figure 8. Schematic diagram the thermal dehydration of pure iron oxyhydroxides to iron oxides.

Conclusions

The IR spectra in the OH group region has been used to follow the formation of iron oxyhydroxides species in a silica xerogel matrix obtained when is used as precursor of iron oxides: nitrate and chloride salts and Fe nanoparticles chemically synthesised.

We observed that under heat treatment the oxyhydroxides species transform to iron oxides species and the magnetic properties suffer evident changes in relationship with these transformation of phase.

The thermal dehydration of pure iron oxyhydroxides to iron oxides showing that α and γ forms of iron oxyhydroxides on thermal dehydration transform into hematite and

maghemite, respectively, whereas the β form transform to the ϵ -Fe₂O₃ without going through an intermediate iron oxide phase. The combination of α form oxyhydroxide with maghemite phase conduce to hematite.

Acknowledgments

This work was done under the auspices of CONACyT (Mexico) through grants G-25851-E and W-8001 (Millennium Initiative).

References

1. R.D. McMichael, R.D. Shull, L.J. Swartzendruber, L.H. Bennett, and R.E. Watson, *J. Magn. Mater.* 111, 29 (1992).
2. C. Cannas, D. Gatteschi, A. Musinu, G. Piccaluga, and C. Sangregorio, *J. Phys. Chem. B* 102, 7721 (1998).
3. F. del Monte, M.P. Morales, D. Levy, A. Fernández, M. Ocaña, A. Roige, E. Molins, K. O'Grady, and, C.J. Cerna, *Langmuir* 13, 3627 (1997).
4. D. Niznansky, N. Viart, and J.L. Rehspringer, *J. Sol-Gel Sci & Tech.* 8, 615 (1997).
5. E.J.A. Pope and J. Mackenzie, *J. Non-Cryst. Solids* 87, 185 (1986).
6. C.J. Brinker and G.W. Scherer, *Sol Gel Science* (Academic Press, San Diego, 1990).
7. R. Cornell and U. Schwertmann, *The Iron Oxides* (VCH, Weinheim, 1996).
8. D.L. Leslie-Pelecky and R.D. Rieke, *Chem. Mater.* 8, 1770

- (1996).
9. J. Yan, A.M. Buckley, and M. Greenblatt, *J. Non-Cryst. Solids* 180, 180 (1995).
 10. S. Ponce-Castañeda, J.R. Martínez, S.A. Palomares-Sánchez, F. Ruiz, and O. Domínguez, *J. Sol-Gel Sci & Tech.* 25, 29 (2002).
 11. T. Ishikawa, W.Y. Cai, and K. Kandori, *J. Chem. Soc., Faraday Trans.* 88, 1173 (1992).
 12. Y. Ryskin, in *The Infrared Spectra of Minerals*, edited by V.C. Farmer (Mineralogical Society, London, 1974) pp. 137, 181.
 13. R. Morris, H. Lauer, Ch. Lawson, E. Gibson, G. Nace, and Ch. Stewart, *J. Geophys. Res.* 90, 3126 (1985).
 14. S. Ramesh, I. Felner, Y. Koltypin, and A. Gedanken, *J. Mater. Res.* 15, 944 (2000).
 15. S. Ponce-Castañeda, J.R. Martínez, F. Ruiz, S.A. Palomares-Sánchez, and J.A. Matutes-Aquino, *J. Magn. Magn. Mater.* 250, 160 (2002).
 16. C. M. Parler, J.A. Ritter, and M.D. Amiridis, *J. Non-Cryst. Solids* 279, 119 (2001).